

# Textural characteristics of sulphided hydrotreatment catalysts prepared using Co–Mo complex compounds

K. A. Leonova · O. V. Klimov · E. Yu. Gerasimov ·  
P. P. Dik · V. Yu. Pereyma · S. V. Budukva ·  
A. S. Noskov

Received: 29 October 2012 / Accepted: 4 February 2013 / Published online: 13 February 2013  
© Springer Science+Business Media New York 2013

**Abstract** Sulphided Co–Mo catalysts prepared by supporting  $(\text{CoL})_2[\text{Mo}_4(\text{C}_6\text{H}_5\text{O}_7)_2\text{O}_{11}] \cdot x\text{H}_2\text{O}$  on  $\gamma\text{-Al}_2\text{O}_3$  were studied. Pores with diameters less than 40 Å in the catalysts preliminary dried at 120 °C were observed. The volume of these pores is proportional to the amount of carbon-containing decomposition products of the citrate ligands. No narrow pores in preliminary calcined catalysts were observed, whereas a sulphided active component was uniformly distributed in pores with diameters greater than 50 Å, independent of the active-metal concentration. The morphology of the active component particles depends on the conditions of the heat pretreatment. Catalysts that contain particles with an average of  $2.1 \pm 0.2$  layers in a stack and pores with diameters of 60–120 Å are the most active in the hydrotreatment of diesel fuels.

**Keywords** Hydrotreating · Localisation of active compound · Micropores

## 1 Introduction

One composition of widely used hydrotreatment catalysts supported on  $\gamma\text{-Al}_2\text{O}_3$  comprises highly dispersed  $\text{MoS}_2(\text{WS}_2)$  particles decorated with Co or Ni atoms. The sulphided active component is often referred to as a Co(Ni)–Mo(W)–S phase in the literature (Topsøe et al. 1979, 1984; Topsøe 2007). Over the last few years, the

most active catalysts that contain the fully sulphided Co(Ni)–Mo(W)–S phase of Type II, which is high active and has no interaction with the support, have been prepared via the impregnation of a carrier using impregnating solutions that contain salts of active metals and different chelating agents (Blanchard et al. 1995; Rinaldi et al. 2010; Al-Dalama and Stanislaus 2006; Shimizu et al. 1998; Sun et al. 2003; Kubota et al. 2010). The catalysts are subsequently dried at temperatures less than the ligand decomposition temperature and are sulphided. The addition of chelating agents into impregnating solutions has been shown to result in the formation of bimetallic complexes (van Veen et al. 1984; Klimov et al. 2010a; Cabello et al. 2000; Nicosia and Prins 2005; Lamonier et al. 2007). Bimetallic complexes with a Mo/Co atomic ratio of 2 are optimal precursors for the sulphided active component, whereas the active metals, i.e., Co and Mo, in these compounds are in close proximity to each other and have the same atomic ratio as the active component (Klimov et al. 2010b; Pashigreva et al. 2010a). The properties of complex compounds result in the formation of a bimetallic Co–Mo–S phase. Chelating agents stabilise complexes in a solution and on a support surface up to the sulphidation stage and decrease undesirable interactions between the active metals and the support (Nicosia and Prins 2005; Sun et al. 2003), which allows the active component with an optimal structure, composition and morphology to be selectively synthesised. In addition to depending on the properties of the Co–Mo–S phase, the catalytic activity also strongly depends on the textural characteristics of catalysts, including the average surface area  $S$ , the pore volume  $V$ , the pore diameter  $D$  and the pore size distribution. These parameters are governed by the characteristics of the initial supports. The geometric size of sulphur-containing molecules, which prevail in hydrotreating feedstocks, depends

K. A. Leonova (✉) · O. V. Klimov · E. Yu. Gerasimov ·  
P. P. Dik · V. Yu. Pereyma · S. V. Budukva · A. S. Noskov  
Boreskov Institute of Catalysis, Siberian Branch,  
Russian Academy of Sciences, Pr. ak. Lavrentiev 5,  
630090 Novosibirsk, Russia  
e-mail: lakmallow@catalysis.ru

on the boiling range of the feed (Song and Ma 2003; Song 2003). Accordingly, wide porous supports should be used for heavier fuels (Rana et al. 2004, 2007). Moreover, the catalyst should contain primarily single-sized pores that are optimal for the specific type of fuel. It is also necessary that the base amount of the active component be exactly localised in pores with an optimal diameter (Klimov et al. 2010c). For example, the presence of the active component localised in pores with diameters less than or equal to 40 Å is not desirable for hydrotreating catalysts of diesel fuels because the active component is not available for substituted dibenzothiophenes, whose transformation is the main goal of the hydrotreatment of diesel fuels.

In the present work, sulphided Co–Mo catalysts prepared by supporting  $(\text{CoL})_2[\text{Mo}_4(\text{C}_6\text{H}_5\text{O}_7)_2\text{O}_{11}] \cdot x\text{H}_2\text{O}$  (Klimov et al. 2010a) on two industrial samples of  $\gamma\text{-Al}_2\text{O}_3$ , which possessed different textural characteristics, were studied. The catalysts were tested in the hydrotreatment of straight-run gas oil. The dependence of the morphology of the sulphided active component on the active-metal concentration and on the heat treatment conditions prior to sulphiding were studied using HRTEM. The textural characteristics of the sulphided catalysts were studied using the nitrogen adsorption method, and the influence of the heat pretreatment conditions, the CoMoCitrate concentration and the texture of the initial supports was defined. The data concerning the morphology of the sulphided particles and the localisation of the active component in the catalysts were correlated with the catalytic-activity data.

## 2 Experimental

### 2.1 Carriers

Samples of  $\gamma\text{-Al}_2\text{O}_3$  produced by Sasol GmbH (Germany) and JSC Promyshlennye Katalizatory (Ryazan, Russia) were used as supports (Table 1). The  $\gamma\text{-Al}_2\text{O}_3$  was granulated in the form of trilobe extrudates with a diameter 1.5 mm. All of the supports were preliminary calcined in air at 550 °C for 4 h.

**Table 1** Textural characteristics of supports

Designation	Average surface area ( $\text{m}^2/\text{g}$ )	Pore volume ( $\text{cm}^3/\text{g}$ )	Average pore diameter (Å)
Al-1 <sup>a</sup>	217	0.75	138
Al-2 <sup>b</sup>	216	0.51	94

<sup>a</sup> The  $\gamma\text{-Al}_2\text{O}_3$  produced by JSC Promyshlennye Katalizatory (Ryazan, Russia). Initial pseudoboehmite was prepared by gibbsite alkaline precipitation

<sup>b</sup> The  $\gamma\text{-Al}_2\text{O}_3$  from Sasol GmbH (Germany) was prepared using alkoxide technology

**Table 2** Characteristics of the catalysts

Names	Carriers	Drying conditions (°C–h)	Metal content (%) <sup>a</sup>
CoMoCitrateS-Al-1	Al-1	120–5	Co 3.0, Mo 10.7 Co 2.0, Mo 7.8
CoMoCitrateOS-Al-1	Al-1	120–5, 550–5	Co 2.4, Mo 5.1 Co 0.9, Mo 3.1
CoMoCitrateS-Al-2	Al-2	120–5	Co 3.0, Mo 9.3 Co 2.4, Mo 7.7
CoMoCitrateOS-Al-2	Al-2	120–5, 550–5	Co 2.6, Mo 5.3 Co 1.1, Mo 3.6

<sup>a</sup> Analysis data for the samples calcined at 550 °C

### 2.2 Preparation of the catalysts

Catalysts were prepared by impregnation of the carriers with an aqueous solution that contained  $(\text{CoL})_2[\text{Mo}_4(\text{C}_6\text{H}_5\text{O}_7)_2\text{O}_{11}] \cdot x\text{H}_2\text{O}$  (hereinafter referred to as CoMoCitrate). The CoMoCitrate complex was synthesised according to the technique described in the literature (Klimov et al. 2010b). Impregnating solutions with concentrations of the complex that resulted in catalysts with a Mo content of 10.0 %, 7.5 %, 5.0 % or 2.5 % and a proportional amount of Co were used. After impregnation, all the catalysts were dried at 120 °C for 5 h or were dried and then calcined at 550 °C for 5 h. After drying, the catalysts were crushed to a particle size 0.25–0.5 mm. The sulphidation of the catalysts in batches of 4 g was performed in  $\text{H}_2\text{S}$  flowing at 1,200 ml/h for 2 h at 220 °C and then for 2 h at 400 °C. The designations of the catalysts, the metal content and the heat treatment conditions before sulphidation are shown in Table 2.

### 2.3 Investigation techniques

Textural properties of the catalysts and supports were determined by nitrogen physisorption using an ASAP 2400 (USA) instrument. Prior to analysis, samples were heated under flowing  $\text{N}_2$  at 200 °C for 2 h. BET surface areas were calculated from the amount of nitrogen uptaken at relative pressures that ranged from 0.05 to 0.30. The total pore volume was derived from the amount of nitrogen adsorbed at a relative pressure close to unity (in practice,  $P/P^0 = 0.995$ ) under the assumption that all of the accessible pores had been filled with condensed nitrogen in the normal liquid state. The pore size distribution was calculated according to the BJH method using the adsorption and desorption branches of the isotherm.

HCNS analysis was performed using a Vario EL III elemental analyser (ELEMENTAR Analysensysteme GmbH).

HRTEM images were obtained on a JEM-2010 electron microscope (JEOL, Japan) with a lattice-fringe resolution of 0.14 nm and operated at an accelerating voltage of 200 kV. The high-resolution images of periodic structures were analysed by the Fourier method. Samples to be examined by HRTEM were prepared on a perforated carbon film mounted on a copper grid. The particle length of the sulphided active component and the stacking number were determined based on the average data for more than 500 particles that were selected from typical patterns for each sample.

Catalysts were tested in the hydrodesulphurisation of straight-run gas oil that contained 1.05 wt% S. The experiment was performed in a plug stainless steel reactor at 3.5 MPa,  $T = 345\text{ }^{\circ}\text{C}$ , a liquid hourly space velocity of  $2\text{ h}^{-1}$  and an  $\text{H}_2$ /feed volume ratio of 300. The sulphur content in the liquid products was measured using a Horiba SLFA-2100 X-ray fluorescence analyser.

### 3 Results and discussion

#### 3.1 Catalytic properties and morphology of sulphided active component particles

CoMoCitrate catalysts supported on  $\gamma\text{-Al}_2\text{O}_3$  samples dried in the range of  $110\text{--}220\text{ }^{\circ}\text{C}$  before sulphidation have been previously reported to exhibit maximum activity in the hydrotreatment of diesel fuels (Pashigreva et al. 2010b). The catalytic activity decreases considerably with increasing drying temperature. Accordingly, in the present work, the catalysts were dried at  $120\text{ }^{\circ}\text{C}$  to ensure high activity due to both the optimal structure of the sulphided active component and the fact that catalysts calcined before sulphidation at  $550\text{ }^{\circ}\text{C}$  would exhibit low activity. The catalytic-activity results with respect to the hydrotreatment of straight-run gas

oil using catalysts that contained 10 % Mo are given in Table 3.

Catalysts calcined prior to sulphidation are considerably less active than catalysts dried at  $120\text{ }^{\circ}\text{C}$ . Independent of the pretreatment conditions, the samples supported on the Al-2 carrier, whose pore diameters mostly fall within the  $50\text{--}130\text{ }\text{\AA}$  range, are more active (Table 1; Figs. 3, 7). Obviously, these pores provide optimal access of the sulphur-containing reagents to the active component and allow the catalyst to possess a high active-metal concentration per unit volume. The Al-1 carrier exhibits a wider pore size distribution (Table 1; Figs. 2, 6). Pores with a diameter less than  $50\text{ }\text{\AA}$  are not available for catalysis, whereas pores with a diameter greater than  $150\text{ }\text{\AA}$  result in a decrease in the active-metal concentration per catalyst volume, which is in good agreement with the literature data (Rana et al. 2004). Thus, in all of the studied cases, the preparation method of the support does not considerably influence the morphology of the sulphide active component particles.

According to the elemental analysis results (Table 4), the S/Mo atomic ratio in all the sulphided catalysts exceeds the ratio necessary for the formation of the sulphided active component that corresponds to the gross formula  $\text{CoMo}_2\text{S}_4$ . The nature of this excess is not clear and is not the subject of the present work. However, the obtained data indicate that full sulphidation of the active metals was achieved in the compositions of all the studied catalysts and that the highly active Co–Mo–S phase of Type II formed, which is in agreement with previous catalysis experiments (Pashigreva et al. 2010b).

The electron microscopy images (Fig. 1) show that the catalysts contain particles of the sulphide active component uniformly distributed on the support surface. Microphotographs that coincide well with those repeatedly described in the literature for Co–Mo–S phase of Type II (Günter

**Table 3** Residual sulphur content in liquid products obtained during the hydrotreatment of straight-run gas oil at  $345\text{ }^{\circ}\text{C}$ , 3.5 MPa, liquid hourly space velocity of  $2\text{ h}^{-1}$  and a  $\text{H}_2$ /feed ratio  $300\text{ nm}^3/\text{m}^3$

Catalyst	CoMoCitrateS-Al-1	CoMoCitrateOS-Al-1	CoMoCitrateS-Al-2	CoMoCitrateOS-Al-2
Residual sulphur content (ppm)	50	180	40	150

**Table 4** HCNS-analysis data for CoMoCitrateS(OS)-Al-1 and CoMoCitrateS(OS)-Al-2 samples

	CoMoCitrateS-Al-1(CoMoCitrateS-Al-2)/CoMoCitrateOS-Al-1(CoMoCitrateOS-Al-2)			
Mo (%)	10.0	7.5	5.0	2.5
N	0.71(0.46)/0.02(0.00)	0.47(0.32)/0.01(0.01)	0.31(0.26)/0.01(0.00)	0.15(0.13)/0.01(0.02)
C	2.63(2.41)/0.03(0.05)	2.00(1.90)/0.04(0.04)	1.59(1.40)/0.05(0.03)	1.04(0.68)/0.06(0.02)
S	8.53(8.69)/12.35(10.71)	8.81(8.72)/9.52(9.36)	6.46(6.30)/6.13(6.22)	4.34(4.60)/3.99(4.12)
H	0.23(0.33)/0.23(0.37)	0.21(0.30)/0.20(0.32)	0.20(0.32)/0.21(0.33)	0.21(0.28)/0.25(0.30)

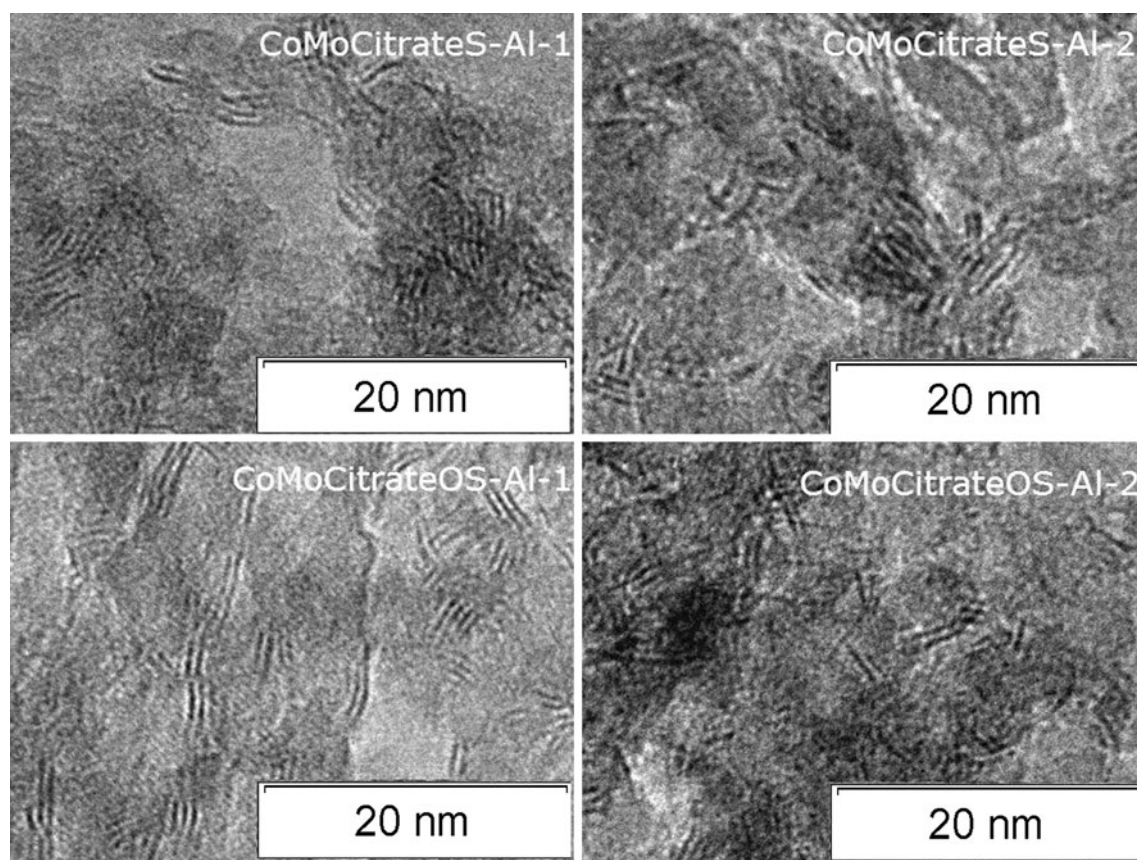


**Fig. 1** HRTEM microphotographs for CoMoCitrateS-Al-1, CoMoCitrateOS-Al-1, CoMoCitrateS-Al-2 and CoMoCitrateOS-Al-2 catalysts

et al. 1988) were obtained for all of the catalysts. They do not indicate the presence Co- and Mo-containing particles, such as individual cobalt sulphides.

Independent of the cobalt and molybdenum concentration, bimetallic sulphided compounds with similar morphologies, average slab lengths of  $2.60 \pm 0.25$  and average stacking numbers of  $2.1 \pm 0.1$  were formed in the CoMoCitrateS-Al-2 catalyst (Table 5). This morphology of sulphide particles is typical for highly active hydrotreatment catalysts of the latest generation (Eijsbouts et al. 2008). Notably, an increase in the molybdenum concentration from 2.5 to 10 % led to a less than 20 % increase in the number of particles visible in the microphotographs that were oriented perpendicular to the support surface. Obviously, the metal concentration in the catalyst and the

number of particles oriented parallel to the support surface that are not visible in HRTEM microphotographs increase simultaneously. An average slab length  $2.8 \pm 0.3$  nm and an average stacking number  $2.8 \pm 0.4$  were obtained for the previously calcined CoMoCitrateOS-Al-2 catalysts, which are considerably less active in the hydrotreatment (Table 3). Notably, the preferential formation of multilayer active component particles is typical for the catalysts calcined prior to sulphidation. Apparently, multilayer particles are less catalytically active. In the CoMoCitrateOS-Al-2 catalysts there are significantly more visible particles on microphotographs than in those of the non-calcined CoMoCitrateS-Al-2 samples. Therefore, an increase in the stacking number leads to the orientation of particles perpendicular to the support surface. Similar results were

**Table 5** HRTEM data for CoMoCitrateS(OS)-Al-1 and CoMoCitrateS(OS)-Al-2 catalysts

Mo (%)	CoMoCitrateS-Al-1/CoMoCitrateS-Al-2				CoMoCitrateOS-Al-1/CoMoCitrateOS-Al-2			
	10.0	7.5	5.0	2.5	10.0	7.5	5.0	2.5
Slab length (nm)	2.8/2.8	2.9/2.8	2.6/2.6	2.3/2.4	2.4/2.5	2.5/2.5	2.7/2.6	2.8/3.1
Stacking number	1.9/2.0	2.0/2.1	2.0/2.1	2.2/2.2	2.8/3.0	3.0/3.1	2.7/2.5	2.6/2.7
Slab number for 1000 nm <sup>2</sup>	55/61	53/50	48/50	55/53	76/82	88/85	59/61	69/74



**Table 6** Textural characteristics of the catalysts

	Mo (%)	CoMoCitrateS-Al-1/ CoMoCitrateOS-Al-1	CoMoCitrateS-Al-2/ CoMoCitrateOS-Al-2
S, m <sup>2</sup> /g ( $\Delta$ ) <sup>a</sup>	10.0	161(–56)/146(–71)	169(–47)/131(–85)
	7.5	155(–62)/152(–65)	186(–30)/153(–63)
	5.0	165(–52)/167(–50)	190(–26)/153(–63)
	2.5	184(–33)/182(–35)	192(–24)/185(–31)
V, cm <sup>3</sup> /g ( $\Delta$ ) <sup>a</sup>	10.0	0.39(–0.36)/0.45(–0.30)	0.28(–0.23)/0.3(–0.21)
	7.5	0.45(–0.30)/0.49(–0.26)	0.33(–0.18)/0.34(–0.17)
	5.0	0.50(–0.25)/0.55(–0.30)	0.34(–0.17)/0.34(–0.17)
	2.5	0.60(–0.15)/0.63(–0.12)	0.42(–0.09)/0.43(0.08)
D, nm ( $\Delta$ ) <sup>a</sup>	10.0	97(–41)/124(–14)	67(–27)/88(–6)
	7.5	97(–41)/129(–9)	71(–23)/90(–4)
	5.0	121(–17)/133(–5)	71(–23)/88(–6)
	2.5	130(–8)/138(–0)	87(–7)/93(–1)

<sup>a</sup> ( $\Delta$ ): an alteration of the parameter (S, V, D) in comparison with the initial support

obtained for the catalysts supported on Al-1: average slab lengths of  $2.65 \pm 0.25$  and  $2.60 \pm 0.25$  nm and average stacking numbers of  $2.0 \pm 0.2$  and  $2.8 \pm 0.2$  were found for non-calcined CoMoCitrateS-Al-1 and calcined CoMoCitrateOS-Al-1 samples, respectively.

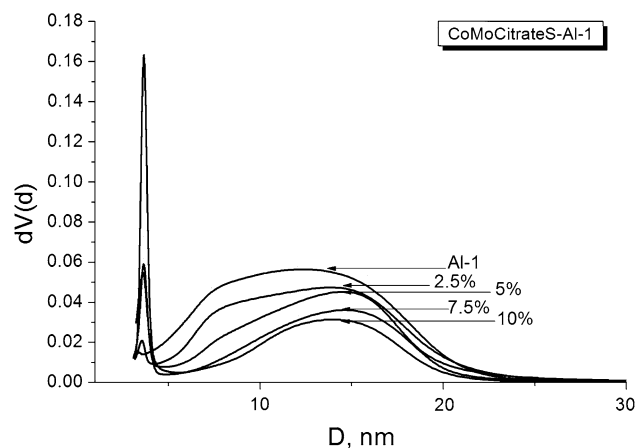
### 3.2 Localisation of the active component in the catalyst and reasons for the formation of secondary pores

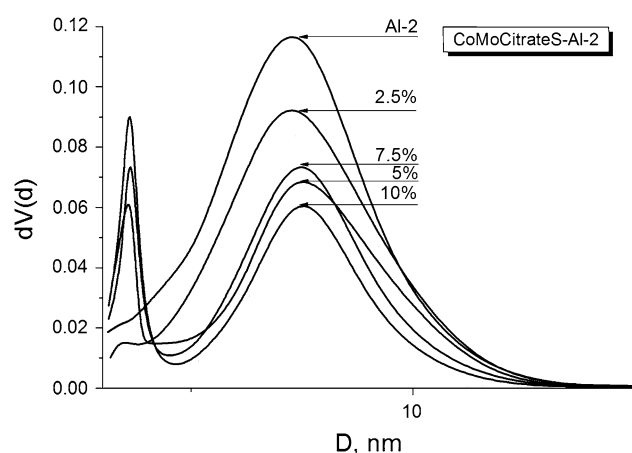
The average surface area, pore volume and pore diameter of studied samples are given in Table 6. In the present work, we used  $\gamma$ -Al<sub>2</sub>O<sub>3</sub>-structured carriers that were preliminary calcined at 550 °C. Therefore, the calcination of the supported catalysts at 550 °C or their sulphidation must not lead to significant sintering and alteration of the textural characteristics of the support, which is consistent with results reported elsewhere (Budukva et al. 2011). Accordingly, all the discrepancies between textural characteristics of the initial supports and those of the studied catalysts are due to the properties of the supported compounds and their concentrations.

Table 6 shows that an increase in the active-metal content leads to monotonic decreases in the average surface area, the pore volume and the pore diameter for all of the studied catalysts. These alterations are attributed to a deposition of Co and Mo on the support surface in the form of sulphided active components and, for the non-calcined samples, of deposition products of citrate ligands formed during the sulphidation stage.

BJH curves for the preliminarily dried and sulphided CoMoCitrateS-Al-1 and CoMoCitrateS-Al-2 samples are shown on Figs. 2 and 3. The corresponding adsorption–desorption isotherms are shown in Figs. 4 and 5. Two groups of changes have been pointed out for these catalysts in comparison with the initial supports: a decrease in the pore volume at 50–200 and at 50–100 Å for the Al-1 and

Al-2 carriers, respectively. Secondary pores are also observed to form. The method used does not allow the precise size and volume of these pores to be determined. However, their diameter most likely does not exceed 40 Å, and their quantity in the catalysts increases in proportion to the supported CoMoCitrate concentration. According to the Brunauer et al. classification (1940), isotherms of the initial supports correspond to Type IV and contain one hysteresis step. The formation of second hysteresis step in the  $P/P^0$  range of 0.4–0.7 (Figs. 4, 5) is observed for the samples that contain  $\geq 5$  % of Mo. At the same time, the shape of the main loop at  $P/P^0 = 0.7$ –1.0 remains unchanged, and its square decreases in proportion to the decrease in the pore volume (Table 6). The formation of secondary narrow pores in the hydrotreating catalysts at different genesis stages have been noted by different authors. Narrow pores were supposed to be produced by coke deposits that contain carbon and nitrogen (Richardson et al. 1996; Wood and Gladden 2003; Vissers et al. 1988) or by particles of sulphided active-metal compounds (Nikulshin et al. 2012).


**Fig. 2** Pore size distribution for CoMoCitrateS-Al-1 samples



**Fig. 3** Pore size distribution for CoMoCitrateS-Al-2 samples

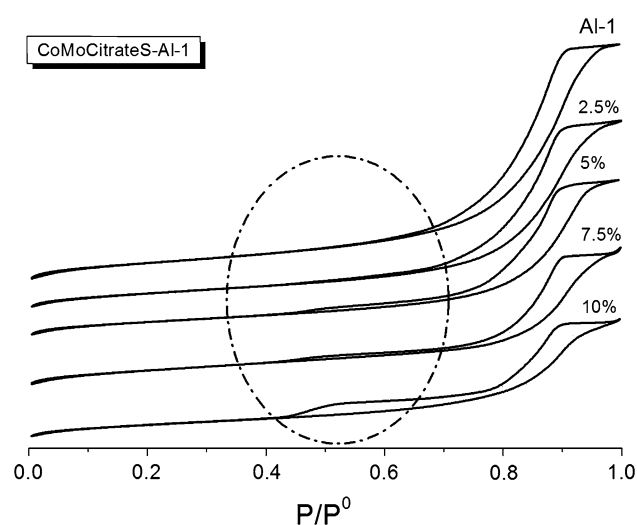


**Fig. 4** Adsorption-desorption isotherms for CoMoCitrateS-Al-1 samples

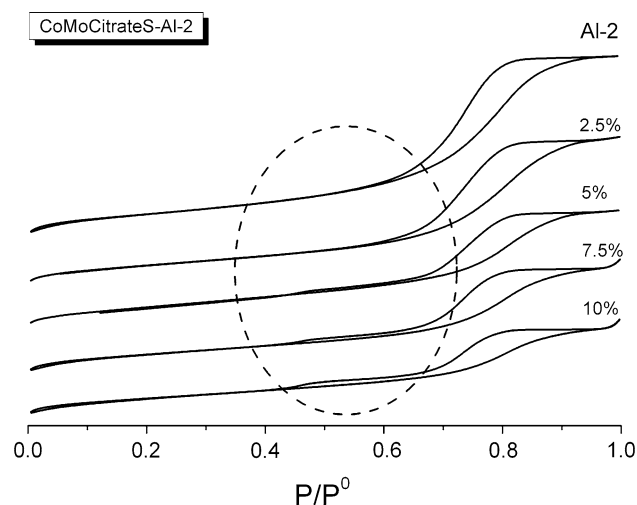


**Fig. 5** Adsorption-desorption isotherms for CoMoCitrateS-Al-2 samples

To understand the reasons for the appearance of narrow pores in our case, catalysts calcined before they were sulphided and without significant amounts of carbon and nitrogen (Table 4) were studied. BJH curves and adsorption-desorption isotherms of these samples are shown in Figs. 6, 7, 8, 9. Independent of the amount of supported metal and the carrier used, no narrow pores formed on the preliminary calcined catalysts, as indicated by the lack of hysteresis loops in the isotherms in the range of  $P/P^0 = 0.4-0.7$ .

The morphology of the sulphided active-component particles in all the studied catalysts is similar (Table 5). However, the calcined catalysts did not contain narrow pores. Therefore, the appearance of narrow pores in non-calcined catalysts is fully accounted for by the formation of carbon deposits during decomposition of the citrate ligands during the sulphiding stage. Sulphided compounds of the active metals do not take part in the formation of secondary pores, irrespective of their concentration in the catalyst. Based on the differences in the average surface area values

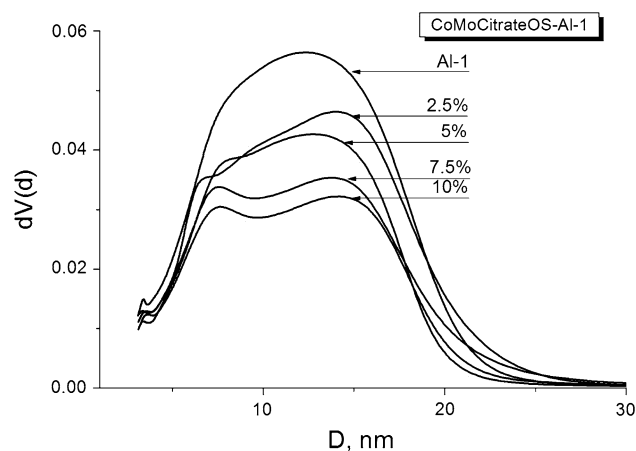


**Fig. 6** Pore size distribution for CoMoCitrateOS-Al-1 samples

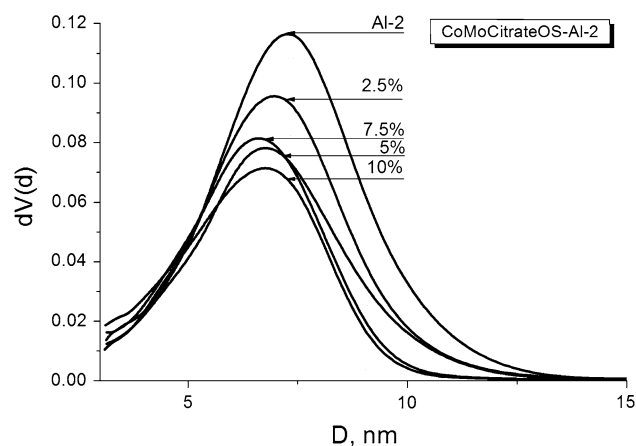


**Fig. 7** Pore size distribution for CoMoCitrateOS-Al-2 samples

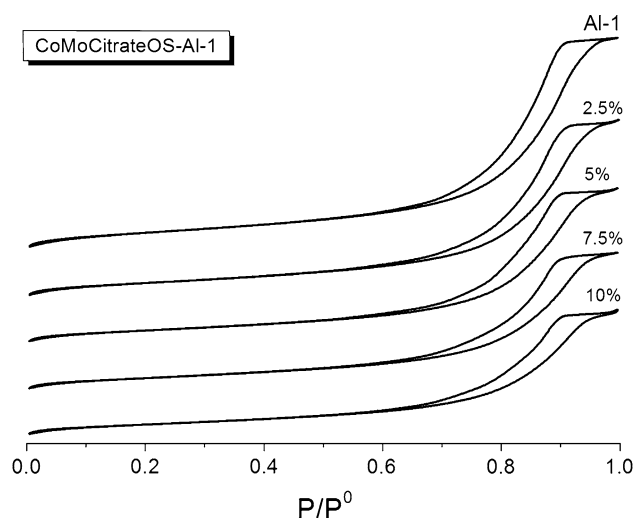


**Fig. 8** Adsorption–desorption isotherms for CoMoCitrateOS-Al-1 samples

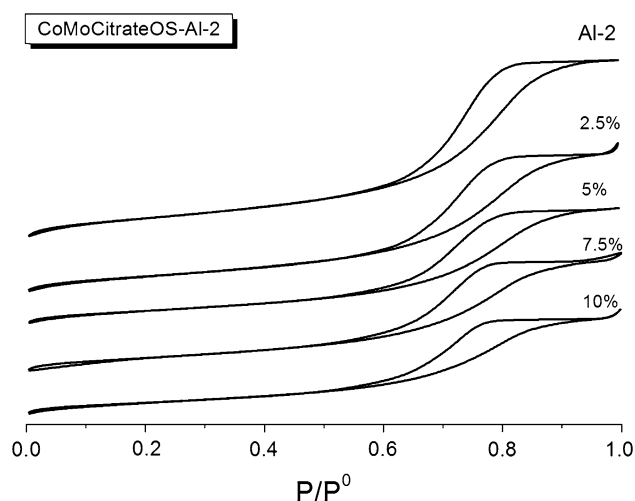


**Fig. 9** Adsorption–desorption isotherms for CoMoCitrateOS-Al-2 samples

for the calcined and non-calcined catalysts supported on the same carrier (Table 6) and on the error calculations, the average surface area of carbon deposits on the catalysts that contain 10 % Mo is approximately  $30 \text{ m}^2$ , and the carbon deposits volume is approximately  $0.03\text{--}0.06 \text{ cm}^3/\text{g}$ . In addition, sulphided compounds of the active component for these catalysts occupy a greater volume: approximately  $0.2\text{--}0.3 \text{ cm}^3/\text{g}$ . Accordingly, in terms of discrepancies between the volumes of definite-sized pores in catalysts with various concentrations of the sulphided active component, conclusions can be drawn about the sulphide active component's preferential localisation in carrier pores, including errors that result from the contributions of carbon deposits in the non-calcined catalysts. However, more precise data on the localisation of the active component can

be obtained from the data for previously calcined catalysts that contain no carbon deposits.

A comparison of changes that occur in the BJH curves (Figs. 2, 6) with increased concentrations of supported metals in the catalysts allows us to conclude that most of the sulphided active component in the catalysts on the Al-1 carrier localises in pores with diameters of  $65\text{--}250 \text{ \AA}$ . The use of impregnation solutions with small CoMoCitrate concentrations leads to the preferential localisation of metals in pores with diameters between  $65$  and  $150 \text{ \AA}$ . An increase in the concentration leads to the filling of wider pores.

For the Al-2 carrier (Figs. 3, 7), a uniform filling of pores with diameters of  $60\text{--}120 \text{ \AA}$  by the active metals occurs when the concentration of active metals in the impregnation solution is increased. In these pores, a major portion of the active metals is localised. Notably, no significant decrease in the volume of pores with diameters less than  $60 \text{ \AA}$  was observed for the previously calcined catalysts supported on both carriers. Obviously, the geometric size of the initial complex (CoMoCitrate), independently of the concentration of the impregnation solutions and, accordingly, independently of the sulphided active component, does not allow it to penetrate into narrow pores, in good agreement with previously published results (Pashigreva et al. 2010c).

For all of the studied cases, no considerable changes in the shapes of the hysteresis loops in the range of  $P/P^0 = 0.7\text{--}1.0$  were observed, except for smooth decreases in their heights that were observed as the concentrations of the supported metals was increased. This behaviour denotes a lack of pore-plugging and indicates a uniform distribution of cobalt and molybdenum on the surfaces of pores, accompanied by a concomitant decrease in the pores' average diameter (Table 6). Notably, a significant decrease was observed in the average pore diameter for non-calcined catalysts compared to that of the calcined catalysts. However, this decrease is associated with the contribution of narrow pores between carbon-deposit particles to the calculated average pore diameter.

All of the changes in the textural characteristics of the supports for CoMoCitrateOS catalysts correspond to the deposition of sulphided active components in the pores. For example, the catalysts that contain 10 % Mo show a decrease in their average pore diameter of  $6\text{--}14 \text{ \AA}$ . The HRTEM data (Fig. 1) indicate a uniform distribution of the sulphided active component on the support surface. The typical degree of visualisation that corresponds to sulphide particles oriented perpendicular to the support surface is known to be approximately  $18\text{--}22 \%$  for hydrotreating catalysts that contain  $3\text{--}7$  molybdenum and  $1.5\text{--}2.5$  cobalt atoms per  $1 \text{ nm}^2$  of surface area (Eijsbouts et al. 1993, 2005). Therefore, a major portion of the Co and Mo atoms

are located in the particles placed parallel to the support surface that contain the active component and that are invisible to HRTEM. In our case, a degree of visualisation and a preferential orientation of the sulphided active-component particles that are parallel to the support surface should be expected for the catalysts with 10 % Mo and 2.5 % Co, which contain approximately 4 Mo and 2 Co atoms per 1 nm<sup>2</sup> of the support; these results are similar to those reported elsewhere (Eijssbouts et al. 1993, 2005).

A surface concentration of 4 Mo and 2 Co atoms per 1 nm<sup>2</sup> in the case of the support with an average surface area of approximately 220 m<sup>2</sup>/g and interatomic Mo–Mo distances of 3.15 Å, which corresponds to the MoS<sub>2</sub> structure (Dickinson and Pauling 1923; Bell and Herfert 1957), have to provide full coverage of the surface by a single-layer of molybdenum disulphide. However, in the studied catalysts, the average number of layers in visible particles of the sulphided active component ranges from 2 to 3 (Table 5). Consequently, a proportional part of the support surface remains uncovered by the active component. Nevertheless, taking into account that the layer thickness of a single MoS<sub>2</sub> slab, based on the available structural data (Dickinson and Pauling 1923; Bell and Herfert 1957), is close to 3.5 Å, the average pore diameter should decrease by approximately 7–10 Å for the catalysts that contain 10 % Mo and 2.5 % Co (4 Mo and 2 Co atoms per 1 nm<sup>2</sup>) at the expense of the localisation of the sulphided active component in the pores. The experimentally determined decrease in the average pore diameter of 14 and 6 Å for the Al-1 and Al-2 carriers (Table 6), respectively, is in good agreement with the calculated results. Thereby the sulphided active component is uniformly distributed on the surfaces of the pores of the supports, which possess pores with diameters greater than 50 Å. This surface distribution of the sulphide active component leads to decreases in the average surface area, the pore volume and the pore diameter that are proportional to the concentration of active metals. Notably, the geometric shape of the pores does not change.

#### 4 Conclusions

The morphology of sulphided active component particles in sulphided catalysts prepared by supporting CoMoCitrate on  $\gamma$ -Al<sub>2</sub>O<sub>3</sub>, the particles' textural characteristics and their activity in the hydrotreatment of diesel fuels depend on the heat pretreatment conditions. The catalysts dried at 120 °C contain pores with diameters less than 40 Å after sulphidation, whereas these pores are absent in the initial supports. The reason for the formation of these pores is the formation of carbon-containing decomposition products of citrate ligands that are formed during sulphidation. These

carbon deposits may result in the formation of active-component particles generated in stacks with an average of  $2.1 \pm 0.2$  layers in the dried and sulphided catalysts. The average number of layers in a stack is significantly higher in preliminary calcined catalysts ( $2.8 \pm 0.3$ ).

Independent of the CoMoCitrate concentration in the impregnation solutions, the sulphided active component is uniformly distributed in pores with diameters greater than 50 Å. Moreover, sulphided active component does not penetrate into narrow pores, and the formation of pores between active component particles was not observed. Thus the discrepancies in the morphologies of sulphided particles are not sufficient to noticeably affect the textural characteristics of the catalysts. Textural characteristics should be strongly influenced by the metal concentration and by their localisation in the specific pores of a support. The activity of the catalysts in the hydrotreatment of diesel fuels depends on the morphology of the sulphided particles, which, in turn, depends on both the heat pretreatment conditions, the textural characteristics of the catalysts and the texture of the support. The catalysts preliminary dried at 120 °C that contain active-component particles with an average of  $2.1 \pm 0.2$  layers in a stack that are localised in pores with diameters of 60–120 Å are the most active in the hydrotreatment of diesel fuels.

#### References

- Al-Dalama, K., Stanislaus, A.: A comparative study of the influence of chelating agents on the hydrodesulfurization (HDS) activity of alumina and silica–alumina-supported CoMo catalysts. *Energy Fuels* **20**(5), 1777–1783 (2006). doi:[10.1021/ef060125a](https://doi.org/10.1021/ef060125a)
- Bell, R.E., Herfert, R.E.: Preparation and characterization of a new crystalline form of molybdenum disulfide. *J. Am. Chem. Soc.* **79**(13), 3351–3354 (1957). doi:[10.1021/ja01570a012](https://doi.org/10.1021/ja01570a012)
- Blanchard, P., Mauchausse, C., Payen, E., Grimblot, J., Poulet, O., Boisdron, N., Loutaty, R.: Preparation and characterization of CoMo/Al<sub>2</sub>O<sub>3</sub> HDS catalysts: effects of a complexing agent. *Stud. Surf. Sci. Catal.* **91**, 1037–1049 (1995). doi:[10.1016/s0167-2991\(06\)81847-1](https://doi.org/10.1016/s0167-2991(06)81847-1)
- Brunauer, S., Deming, L.S., Deming, W.E., Teller, E.: On a theory of the van der Waals adsorption of gases. *J. Am. Chem. Soc.* **62**(7), 1723–1732 (1940). doi:[10.1021/ja01864a025](https://doi.org/10.1021/ja01864a025)
- Budukva, S., Klimov, O., Litvak, G., Chesalov, Y., Prosvirin, I., Larina, T., Noskov, A.: Deactivation and oxidative regeneration of modern catalysts for deep hydropurification of diesel fuel: oxidative regeneration of IK-GO-1 catalyst. *Russ. J. Appl. Chem.* **84**(1), 95–102 (2011). doi:[10.1134/s1070427211010162](https://doi.org/10.1134/s1070427211010162)
- Cabello, C.I., Botto, I.L., Thomas, H.J.: Anderson type heteropolyoxomolybdates in catalysis: 1. (NH<sub>4</sub>)<sub>3</sub>[CoMo<sub>6</sub>O<sub>24</sub>H<sub>6</sub>]·7H<sub>2</sub>O/ $\gamma$ -Al<sub>2</sub>O<sub>3</sub> as alternative of Co–Mo/ $\gamma$ -Al<sub>2</sub>O<sub>3</sub> hydrotreating catalysts. *Appl. Catal. A* **197**(1), 79–86 (2000). doi:[10.1016/s0926-860x\(99\)00535-9](https://doi.org/10.1016/s0926-860x(99)00535-9)
- Dickinson, R.G., Pauling, L.: The crystal structure of molybdenite. *J. Am. Chem. Soc.* **45**(6), 1466–1471 (1923). doi:[10.1021/ja01659a020](https://doi.org/10.1021/ja01659a020)



- Eijssbouts, S., Heinerman, J.J.L., Elzerman, H.J.W.: MoS<sub>2</sub> structures in high-activity hydrotreating catalysts: I. Semi-quantitative method for evaluation of transmission electron microscopy results. Correlations between hydrodesulfurization and hydrodenitrogenation activities and MoS<sub>2</sub> dispersion. *Appl. Catal. A* **105**(1), 53–68 (1993). doi:[10.1016/0926-860x\(93\)85133-a](https://doi.org/10.1016/0926-860x(93)85133-a)
- Eijssbouts, S., van den Oetelaar, L.C.A., van Puijenbroek, R.R.: MoS<sub>2</sub> morphology and promoter segregation in commercial Type 2 Ni–Mo/Al<sub>2</sub>O<sub>3</sub> and Co–Mo/Al<sub>2</sub>O<sub>3</sub> hydroprocessing catalysts. *J. Catal.* **229**(2), 352–364 (2005). doi:[10.1016/j.jcat.2004.11.011](https://doi.org/10.1016/j.jcat.2004.11.011)
- Eijssbouts, S., Battiston, A.A., van Leerdam, G.C.: Life cycle of hydroprocessing catalysts and total catalyst management. *Catal. Today* **130**(2–4), 361–373 (2008). doi:[10.1016/j.cattod.2007.10.112](https://doi.org/10.1016/j.cattod.2007.10.112)
- Günter, J.R., Marks, O., Korányi, T.I., Paál, Z.: High-resolution electron microscopy of cobalt–molybdenum catalysts structural changes and activity. *Appl. Catal.* **39**, 285–294 (1988). doi:[10.1016/s0166-9834\(00\)80955-0](https://doi.org/10.1016/s0166-9834(00)80955-0)
- Klimov, O.V., Pashigreva, A.V., Bukhtiyarova, G.A., Budukva, S.V., Fedotov, M.A., Kochubey, D.I., Chesalov, Y.A., Zaikovskii, V.I., Noskov, A.S.: Bimetallic Co–Mo complexes: a starting material for high active hydrodesulfurization catalysts. *Catal. Today* **150**(3–4), 196–206 (2010a). doi:[10.1016/j.cattod.2009.07.095](https://doi.org/10.1016/j.cattod.2009.07.095)
- Klimov, O.V., Pashigreva, A.V., Fedotov, M.A., Kochubey, D.I., Chesalov, Y.A., Bukhtiyarova, G.A., Noskov, A.S.: Co–Mo catalysts for ultra-deep HDS of diesel fuels prepared via synthesis of bimetallic surface compounds. *J. Mol. Catal. A* **322**(1–2), 80–89 (2010b). doi:[10.1016/j.molcata.2010.02.020](https://doi.org/10.1016/j.molcata.2010.02.020)
- Klimov, O.V., Pashigreva, A.V., Leonova, K.A., Bukhtiyarova, G.A., Budukva, S.V., Noskov, A.S.: Bimetallic Co–Mo-complexes with optimal localization on the support surface: a way for highly active hydrodesulfurization catalysts preparation for different petroleum distillates. *Stud. Surf. Sci. Catal.* **175**, 509–512 (2010c). doi:[10.1016/s0167-2991\(10\)75096-5](https://doi.org/10.1016/s0167-2991(10)75096-5)
- Kubota, T., Rinaldi, N., Okumura, K., Honma, T., Hirayama, S., Okamoto, Y.: In situ XAFS study of the sulfidation of Co–Mo/B<sub>2</sub>O<sub>3</sub>/Al<sub>2</sub>O<sub>3</sub> hydrodesulfurization catalysts prepared by using citric acid as a chelating agent. *Appl. Catal. A* **373**(1–2), 214–221 (2010). doi:[10.1016/j.apcata.2009.11.023](https://doi.org/10.1016/j.apcata.2009.11.023)
- Lamonier, C., Martin, C., Mazurelle, J., Harlé, V., Guillaume, D., Payen, E.: Molybdocobaltate cobalt salts: new starting materials for hydrotreating catalysts. *Appl. Catal. B* **70**(1–4), 548–556 (2007). doi:[10.1016/j.apcatb.2005.12.027](https://doi.org/10.1016/j.apcatb.2005.12.027)
- Nicosia, D., Prins, R.: The effect of glycol on phosphate-doped CoMo/Al<sub>2</sub>O<sub>3</sub> hydrotreating catalysts. *J. Catal.* **229**(2), 424–438 (2005). doi:[10.1016/j.jcat.2004.11.014](https://doi.org/10.1016/j.jcat.2004.11.014)
- Nikulshin, P.A., Mozhaev, A.V., Pimerzin, A.A., Kononov, V.V., Pimerzin, A.A.: CoMo/Al<sub>2</sub>O<sub>3</sub> catalysts prepared on the basis of Co<sub>2</sub>Mo<sub>10</sub>-heteropolyacid and cobalt citrate: effect of Co/Mo ratio. *Fuel* **100**, 24–33 (2012). doi:[10.1016/j.fuel.2011.11.028](https://doi.org/10.1016/j.fuel.2011.11.028)
- Pashigreva, A.V., Klimov, O.V., Bukhtiyarova, G.A., Fedotov, M.A., Kochubey, D.I., Chesalov, Y.A., Zaikovskii, V.I., Prosvirin, I.P., Noskov, A.S.: The superior activity of the CoMo hydrotreating catalysts, prepared using citric acid: what's the reason?. *Stud. Surf. Sci. Catal.* **175**, 109–116 (2010a). doi:[10.1016/s0167-2991\(10\)75014-x](https://doi.org/10.1016/s0167-2991(10)75014-x)
- Pashigreva, A.V., Bukhtiyarova, G.A., Klimov, O.V., Chesalov, Y.A., Litvak, G.S., Noskov, A.S.: Activity and sulfidation behavior of the CoMo/Al<sub>2</sub>O<sub>3</sub> hydrotreating catalyst: the effect of drying conditions. *Catal. Today* **149**(1–2), 19–27 (2010b). doi:[10.1016/j.cattod.2009.07.096](https://doi.org/10.1016/j.cattod.2009.07.096)
- Pashigreva, A.V., Klimov, O.V., Bukhtiyarova, G.A., Kochubey, D.I., Prosvirin, I.P., Chesalov, Y.A., Zaikovskii, V.I., Noskov, A.S.: High-active hydrotreating catalysts for heavy petroleum feeds: intentional synthesis of CoMo sulfide particles with optimal localization on the support surface. *Catal. Today* **150**(3–4), 164–170 (2010c). doi:[10.1016/j.cattod.2009.08.021](https://doi.org/10.1016/j.cattod.2009.08.021)
- Rana, M.S., Ancheyta, J., Rayo, P., Maity, S.K.: Effect of alumina preparation on hydrodemetallization and hydrodesulfurization of Maya crude. *Catal. Today* **98**(1–2), 151–160 (2004). doi:[10.1016/j.cattod.2004.07.029](https://doi.org/10.1016/j.cattod.2004.07.029)
- Rana, M.S., Capitaine, E.M.R., Leyva, C., Ancheyta, J.: Effect of catalyst preparation and support composition on hydrodesulfurization of dibenzothiophene and Maya crude oil. *Fuel* **86**(9), 1254–1262 (2007). doi:[10.1016/j.fuel.2006.09.015](https://doi.org/10.1016/j.fuel.2006.09.015)
- Richardson, S.M., Nagaishi, H., Gray, M.R.: Initial coke deposition on a NiMo/γ-Al<sub>2</sub>O<sub>3</sub> bitumen hydroprocessing catalyst. *Ind. Eng. Chem. Res.* **35**(11), 3940–3950 (1996). doi:[10.1021/ie950761o](https://doi.org/10.1021/ie950761o)
- Rinaldi, N., Kubota, T., Okamoto, Y.: Effect of citric acid addition on the hydrodesulfurization activity of MoO<sub>3</sub>/Al<sub>2</sub>O<sub>3</sub> catalysts. *Appl. Catal. A* **374**(1–2), 228–236 (2010). doi:[10.1016/j.apcata.2009.12.015](https://doi.org/10.1016/j.apcata.2009.12.015)
- Shimizu, T., Hiroshima, K., Honma, T., Mochizuki, T., Yamada, M.: Highly active hydrotreatment catalysts prepared with chelating agents. *Catal. Today* **45**(1–4), 271–276 (1998). doi:[10.1016/S0920-5861\(98\)00227-2](https://doi.org/10.1016/S0920-5861(98)00227-2)
- Song, C.: An overview of new approaches to deep desulfurization for ultra-clean gasoline, diesel fuel and jet fuel. *Catal. Today* **86**(1–4), 211–263 (2003). doi:[10.1016/s0920-5861\(03\)00412-7](https://doi.org/10.1016/s0920-5861(03)00412-7)
- Song, C., Ma, X.: New design approaches to ultra-clean diesel fuels by deep desulfurization and deep dearomatization. *Appl. Catal. B* **41**(1–2), 207–238 (2003). doi:[10.1016/s0926-3373\(02\)00212-6](https://doi.org/10.1016/s0926-3373(02)00212-6)
- Sun, M., Nicosia, D., Prins, R.: The effects of fluorine, phosphate and chelating agents on hydrotreating catalysts and catalysis. *Catal. Today* **86**(1–4), 173–189 (2003). doi:[10.1016/s0920-5861\(03\)00410-3](https://doi.org/10.1016/s0920-5861(03)00410-3)
- Topsøe, H.: The role of Co–Mo–S type structures in hydrotreating catalysts. *Appl. Catal. A* **322**, 3–8 (2007). doi:[10.1016/j.apcata.2007.01.002](https://doi.org/10.1016/j.apcata.2007.01.002)
- Topsøe, H., Candia, R., Burriesci, N., Clausen, B.S., Mørup, S.: The influence of the support on Co–Mo hydrodesulfurization catalysts. *Stud. Surf. Sci. Catal.* **3**, 479–492 (1979). doi:[10.1016/s0167-2991\(09\)60231-7](https://doi.org/10.1016/s0167-2991(09)60231-7)
- Topsøe, H., Candia, R., Topsøe, N.-Y., Clausen, B.S., Topsøe, H.: On the state of the Co–Mo–S model. *Bull. Soc. Chim. Belg.* **93**(8–9), 783–806 (1984). doi:[10.1002/bscb.19840930820](https://doi.org/10.1002/bscb.19840930820)
- van Veen, J.A.R., Gerkema, E., van der Kraan, A.M., Knoester, A.: A real support effect on the activity of fully sulphided CoMoS for the hydrodesulphurization of thiophene. *J. Chem. Soc. Chem. Commun.* **22**, 1684–1686 (1987)
- Vissers, J.P.R., Mercx, F.P.M., Bouwens, S.M.A.M., de Beer, V.H.J., Prins, R.: Carbon-covered alumina as a support for sulfide catalysts. *J. Catal.* **114**(2), 291–302 (1988). doi:[10.1016/0021-9517\(88\)90033-4](https://doi.org/10.1016/0021-9517(88)90033-4)
- Wood, J., Gladden, L.F.: Effect of coke deposition upon pore structure and self-diffusion in deactivated industrial hydroprocessing catalysts. *Appl. Catal. A* **249**(2), 241–253 (2003). doi:[10.1016/s0926-860x\(03\)00200-x](https://doi.org/10.1016/s0926-860x(03)00200-x)